The permissible calibration error of standard thermocouples with a thermostatted cold junction is 0.16 mV for Chromel−Copel [4]. For a differential thermocouple, we can assume a relative error $\gamma_3 = 1.50\%$ at $\Delta t = 2°K$. Since the transducer will be used in compact equipment, we need not consider the effect of long leads.

Thus, in using the thermoelectric transducer in control systems, i.e., without a recorder, the total relative measurement error will be: $\gamma = \gamma_1 + \gamma_2 + \gamma_3 = 0.00 + 0.61 + 1.50 = 2.11\%$. If the transducer is used with a class 0.5 recorder, the total error of the system in measuring microrates of flow will not exceed 2.11%.

NOTATION

A, coefficient determined in context; c, specific heat; F, cross-sectional area; L, distance between radiator and unit; l, distance between junctions of thermoelectrodes; M, mass flow rate of the liquid metal; S, sensitivity of the transducer; t, temperature; t_{in}, temperature of the flow at the transducer inlet; x, coordinate along the pipe; γ, measurement error; Δ, temperature difference of the thermoelectrode junctions; λ, thermal conductivity. Indices: w, pipe wall; q, liquid metal flow; r, heat-exchanger−radiator.

LITERATURE CITED

1. P. P. Kremlevskii, Flow Meters and Counters [in Russian], Mashinostroenie, Leningrad (1975).
2. P. A. Korotkov and R. K. Azimov, "Thermal-type flow meter for liquid metals," Izv. Vyssh. Uchebn. Zaved., Priborostr., No. 3, 100-103 (1967).
3. V. P. Preobrazhenskii, Heat Engineering Measurements and Instruments [in Russian], Énergiya, Moscow (1978).
4. Yu. V. Safroshkin, Transient Characteristics and Stability of Transistor Voltage and Current Regulators [in Russian], Énergiya, Moscow (1968).

FILM-TYPE THERMOELECTRIC AND THERMOMAGNETIC THERMAL RADIATION SENSORS AND THEIR OUTPUT PARAMETERS

V. V. Borodin, D. M. Gel'fgat, and Z. M. Dashevskii

Voltage−power sensitivity and time constant of a "star"-type film thermoelectric sensor and time constant of a film thermomagnetic sensor are calculated.

Thermal radiation sensors are widely used in thermometry as primary transducers. Their most important output parameters are the conversion coefficient or voltage−power sensitivity and their response time or time constant. In recent years interest has increased in thermal-type sensors, in particular, in film thermoelectric and film thermomagnetic sensors [1, 2]. Such sensors are small in size, reliable in operation, and of high technological quality. Decrease in geometrical dimensions and use of high efficiency film materials permits achievement of high-quality output parameters.

Using two types of film radiation sensor construction (thermoelectric and thermomagnetic), the authors have analyzed the transient thermal processes which occur within the sensor when radiation is incident on the receiver area. The relationships thus obtained have been used to calculate the output parameters of sensors using the most efficient working materials.

One of the most widely used film thermoelectric sensor constructions is the "star" type [1]. The "star" construction (Fig. 1) consists of a substrate 1 in the form of a disk with a film thermobattery 2 deposited on its surface by vacuum technology methods. The branches of the thermobattery have the form of tapered segments which converge at the center, with the gaps between these branches being quite small in comparison

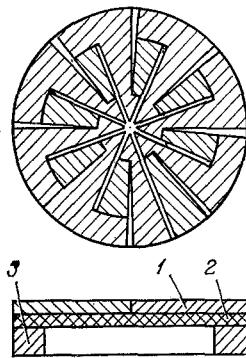Fig. 1   Fig. 2
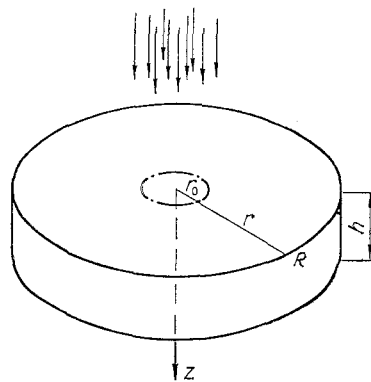
Fig. 1. Construction of "star"-type sensor.

Fig. 2. Model of "star" sensor used in thermal calculation.

to the branch width. The thermobattery cells are connected in series by the overlapping of the branches at the "hot" and "cold" junctions.

The "hot" junctions of the thermobattery are located in the center of the substrate in the receiver area. To thermally stabilize the "cold" junctions the substrate and attached thermobattery are fixed to a massive heat sink 3 about the outer edge.

To calculate the sensor output parameters it is necessary to determine the temperature of the active element, which satisfies the transient thermal conductivity equation

$$\frac{\partial T}{\partial t} = D \Delta T, \tag{1}$$

where $D = \varkappa / cd$.

The sensor construction described above can be represented by a continuous isotropic disk (Fig. 2) with averaged properties, considering the presence of the deposited layer and substrate:

$$cd = \frac{c_1 d_1 h_1 + c_2 d_2 h_2}{h_1 + h_2}, \tag{2}$$

$$\varkappa = \frac{\varkappa_1 h_1 + \varkappa_2 h_2}{h_1 + h_2}. \tag{3}$$

As will be shown below, for film thicknesses $h_1 \leq 10\ \mu m$ the thermal flux propagates along the substrate and semiconductor layer with practically no component across the disk, indicating the validity of the assumption made. It was also assumed that the semiconductor film has ideal contact with the substrate, there being no thermal resistance at the film – substrate boundary. We will also note that the calculation was performed for operation in a vacuum.

The "hot" junctions located in the central area of a disk of radius r_0 are subjected to the action of a constant radiation level beginning at the initial time. The "cold" junctions at the disk edge are maintained at the constant temperature of the surrounding medium T_0. Therefore, the temperature of the lateral disk surface (its rim of radius R) will be assumed given and equal to T_0. For convenience we will use T_0 as a reference point in measuring temperature.

In this case the initial and boundary conditions in cylindrical coordinates r, z appear as follows. At t = 0

$$T(0,\ r,\ z) = 0. \tag{4}$$

On the lateral surface

$$T(t,\ R,\ z) = 0. \tag{5}$$

On the lower surface the thermal flux reaching the surface from the disk volume is equal to the thermal flux radiated from this surface into the surrounding space:

$$\left[\varkappa \frac{\partial T}{\partial z} + 4\varepsilon\sigma T_0^3 T \right]_{z=h} = 0, \tag{6}$$

TABLE 1. Time Constant of "Star"-Type Sensor t_{set}, sec

Substrate	ε	Semiconductor layer thickness h_1, μm											
		0,1			1			5			10		
		Sensor radius R, mm											
		1	3	5	1	3	5	1	3	5	1	3	5
Mica, h_2 = 10 μm	1	0,21	1,02	1,48	0,2	1,02	1,5	0,19	1,04	1,65	0,17	1,06	1,79
	0,2	0,23	1,73	3,67	0,22	1,7	3,65	0,2	1,58	3,57	0,18	1,49	3,5
Polynimide, h_2 = 10 μm	1	0,59	1,26	1,39	0,49	1,25	1,43	0,31	1,23	1,61	0,24	1,22	1,79
	0,2	0,87	4,02	5,66	0,66	3,54	5,43	0,36	2,5	4,77	0,27	2,03	4,35
Semiconductor without substrate	1	0,009	0,0095	0,0096	0,054	0,088	0,093	0,1	0,339	0,42	0,112	0,524	0,74
	0,2	0,035	0,046	0,047	0,10	0,34	0,42	0,12	0,78	1,37	0,124	0,93	1,92

TABLE 2. Voltage–Power Sensitivity S of "Star"–Type Sensor (number of thermoelements m = 8, thermo–emf of single element 3,2 mV/deg K, radius of central irradiated area r_0 = 1 mm), V/W

Substrate	ε	Semiconductor layer thickness h_1, μm											
		0,1			1			5			10		
		Sensor radius R, mm											
		1	3	5	1	3	5	1	3	5	1	3	5
Mica, h_2=10 μm	1	1,00	3,34	3,75	0,94	3,2	3,32	0,72	2,67	2,82	0,56	2,26	2,4
	0,2	1,09	5,4	6,1	1,01	4,82	5,75	0,765	3,75	4,6	0,59	2,94	3,68
Polynimide, h_2=10 μm	1	3,93	7,27	7,27	3,3	6,41	6,43	1,55	4,41	4,46	0,96	3,26	3,37
	0,2	5,68	18,5	18,6	4,05	14,49	15,14	1,75	7,77	8,75	1,04	4,45	5,87
Semiconductor without substrate	1	10,38	11,73	11,74	5,68	8,74	8,74	2,02	5,13	5,15	1,15	3,6	3,7
	0,2	37,1	49,8	49,8	10,1	25,62	25,73	2,41	9,9	10,82	1,24	4,72	6,7

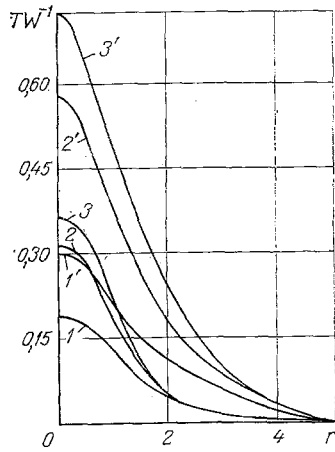Fig. 3   Fig. 4

Fig. 3. Temperature distribution in disk (inner diameter $r_0 = 1$ mm, outer diameter R = 5 mm) for semiconductor thickness $h_1 = 5$ μm: 1) layer on mica, thickness $h_2 = 10$ μm; 2) layer on polynimide, thickness $h_2 = 10$ μm; 3) layer without substrate at z = 0, h/2, h; 1, 2, 3, $\varepsilon = 1$; 1', 2', 3', same as 1, 2, 3 at $\varepsilon = 0.2$. TW^{-1}, deg K·m^2/W; r, mm.
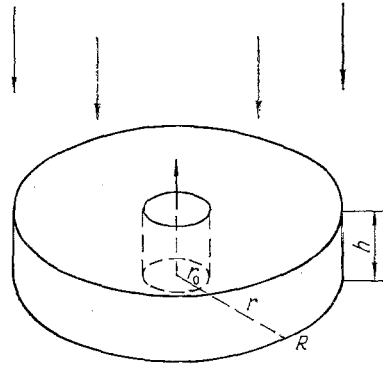
Fig. 4. Model of thermomagnetic sensor used in thermal calculation.

where $h = h_1 + h_2$. On the upper surface the thermal flux incident from the outside on the central portion of the disk of radius r_0 is equal to the algebraic sum of the flux radiated from the surface into the surrounding space and the flux flowing into the volume of the disk:

$$\left[-\varkappa \frac{\partial T}{\partial z} + 4\varepsilon\sigma T_0^3 T \right]_{z=0} = WE(t) E(r_0 - r), \tag{7}$$

where

$$E(t) = \begin{cases} 1 & \text{at} \quad t > 0, \\ 0 & \text{at} \quad t = 0 \end{cases} \text{and } E(r_0 - r) = \begin{cases} 1 & \text{at} \quad r \leqslant r_0, \\ 0 & \text{at} \quad r > r_0. \end{cases}$$

Solution of Eq. (1) with the specified initial and boundary conditions, Eqs. (4)-(7), by the Green's function method revealed that the time dependence of temperature is a complex exponential function. For a disk thickness $h \leq \varkappa/4\varepsilon\sigma T_0^3$ the sensor time constant is given by:

$$t_{set} = \frac{cdhR^2}{8\varepsilon\sigma T_0^3 R^2 + \varkappa x_1^2 h}. \tag{8}$$

The time constant expression, Eq. (8), can be written in the form

$$t_{set} = \frac{C}{G_{rad} + G_{therm}}, \tag{9}$$

where $G = cdh\pi R^2$; $G_{therm} = \varkappa x_1^2 \pi h$, $G_{rad} = 8\varepsilon\sigma T_0^3 \pi R^2$. For $G_{rad} \gg G_{therm}$ $t_{set} \to cdh/8\varepsilon\sigma T_0^3$ and is independent of disk radius. Equation (8) was used to calculate the time constant of a "star"-type sensor for various thicknesses ($h_1 = 0.1$-10 μm) of the most efficient sensor materials, solid solutions $Bi_xSb_{2-x}Te_3$ with p- and n-conductivity.* Substrates were mica or polynimide films 10 μm thick. As is evident from the calculated time constant values (Table 1), for R $\leq$ 5 mm, even for an active layer thickness of 0.1 μm on the mica or polynimide, due to heat transfer by substrate thermal conductivity this case is not realized. The time constant t_{set} ceased to depend on R only in the hypothetical case of absence of the substrate.

For $G_{therm} \gg G_{rad}$, $t_{set} \to dc/\varkappa R^2/x_1^2$ and is independent of ε, and also of h in explicit form. However, in the case of a two-layer film—substrate system increase in the active layer thickness h_1 leads to a change in the effective parameters $\varkappa$ and cd (see Eqs. (2), (3)). At small thicknesses $h_1 = 0.1$ μm $\varkappa$ practically coincides with the substrate thermal conductivity coefficient $\varkappa_2$, and cd $\approx c_2d_2$. Increase in active layer thickness

---

* For solid solutions $Bi_xSb_{2-x}Te_3$ the quantity $\varkappa/4\varepsilon\sigma T_0^3 \approx 25$ cm, so that the condition $h \leq \varkappa/4\varepsilon\sigma T_0^3$ is satisfied.

with use of a polynimide substrate causes an increase in $\varkappa$, and at $h_l \geq 10\ \mu m$, $\varkappa \approx \varkappa_1$. Therefore, in this case, at $R \leq 3$ mm ($G_{therm} > G_{rad}$) the time constant t_{set} decreases with increase in semiconductor layer thickness h_1. When time constants values are compared for semiconductor−mica and semiconductor−polynimide systems, where t_{set} is determined essentially by radiation processes (disk radius $R \geq 3$ mm, $\varepsilon = 1$) t_{set} for a polynimide sensor is less than t_{set} for a mica sensor because the heat capacity of the polynimide is less than that of the mica. When R decreases and $\varepsilon = 0, 2$, i.e., the contribution of G_{therm} increases, the value of the polynimide sensor time constant becomes greater than that of the mica sensor because $\varkappa_{mica}/\varkappa_{polynimide} > (cd)_{mica}/(cd)_{polynimide}$.

The steady-state temperature distribution is determined by the following expression:

$$T(\infty, r, z) = \frac{Wr_0}{2\varepsilon\sigma T_0^3 R} \sum_{n=1}^{\infty} \frac{J_1\left(\frac{x_n}{R} r_0\right) J_0\left(\frac{x_n}{R} r\right)}{x_n J_1^2(x_n)} \times$$
$$\times \frac{\text{sh}\left[\frac{x_n}{R}(h-z)\right] + \frac{x_n \varkappa}{4\varepsilon\sigma T_0^3 R} \text{ch}\left[\frac{x_n}{R}(h-z)\right]}{\left[1 + \left(\frac{x_n \varkappa}{4\varepsilon\sigma T_0^3 R}\right)^2\right] \text{sh}\left(\frac{x_n}{R} h\right) + \frac{x_n \varkappa}{2\varepsilon\sigma T_0^3 R} \text{ch}\left(\frac{x_n}{R} r\right)} .$$
(10)

To determine the voltage−power sensitivity it is necessary to define the temperature of the "hot" junctions (central disk region, averaged over area):

$$\overline{T} = \frac{\int_0^{r_0} T(\infty, r, z) r dr}{\pi r_0^2} = \frac{W}{2\varepsilon\sigma T_0^3} \sum_{n=1}^{\infty} \left[\frac{J_1\left(\frac{x_n r_0}{R}\right)}{x_n J_1(x_n)}\right]^2 \frac{\text{sh}\left[\frac{x_n}{R}(h-z)\right] + \frac{x_n}{R} \text{ch}\left[\frac{x_n}{R}(h-z)\right]}{\left[1 + \left(\frac{x_n \varkappa}{4\varepsilon\sigma T_0^3 R}\right)^2\right] \text{sh}\left(\frac{x_n}{R} h\right) + 2\left(\frac{x_n \varkappa}{4\varepsilon\sigma T_0^3 R}\right)^2 \text{ch}\left(\frac{x_n}{R} h\right)} .$$
(11)

The value of the voltage−power sensitivity S for thermoelectric sensors is given by the expression:

$$S = \frac{m\alpha_{p,n}\Delta T}{WF} .$$
(12)

In the present case $\Delta T = \overline{T}$, while $F = \pi r_0^2$. A computer was used to calculate temperature distributions and voltage−power sensitivity for "star"-type sensors using Eqs. (11), (12). The calculation was performed for the same cases as the time-constant calculations.

To verify the assumption of absence of thermal flux across the disk due to the small active layer thickness $h_l \leq 10\ \mu m$ the temperature distribution over thickness of a semiconductor layer without substrate was also calculated. As is evident from Fig. 3, temperature values over the layer thickness proved identical, which confirms the assumption made. Therefore, for the film−substrate system only the temperature distribution on the disk surface was considered. It is evident from the curves that this distribution is nonlinear. We note that if heat transfer occurred only by thermal conductivity the temperature would change along a branch linearly. The observed temperature distribution is related to the significant contribution of radiant heat transfer. Because of this, at $r \geq 3$ ($\varepsilon = 1$) for both the mica and polynimide sensor the temperature practically attains the "cold" junction temperature. As a result, the voltage−power sensitivity (Table 2) undergoes practically no change for increase in disk radius above 3 mm.

The operation of thermomagnetic sensors is based on the transverse Nernst−Ettingshausen effect in which an electric field E_{N-E} develops in a direction perpendicular to the temperature gradient ∇T and the direction of the magnetic field B:

$$E_{N-E} = Q_\perp B \nabla T.$$
(13)

Important features distinguishing such sensors from thermoelectric ones are the absence of commutation and use of material of a single conductivity type, which permits variation of the working element dimensions over a wide range. For such a sensor the output signal $U_{N-E} = E_{N-E}l$ (where l is the length of the working element) does not depend on the temperature head ΔT as in thermoelectric sensors, but on the temperature gradient ∇T. The voltage−power sensitivity of such a sensor is defined by the expression

$$S = Q_\perp B \nabla T l / WF.$$
(14)

Therefore, when the thermal flux is carried along the working element solely by thermal conductivity, the voltage—power sensitivity is independent of working element height:

$$S \simeq Q_\perp Bl/\varkappa F. \tag{15}$$

This permits reduction in the height of the working element, which leads to a sharp drop in the time constant t_{set} while maintaining the same sensitivity S.

A thermomagnetic sensor construction was developed in which the active element is in the form of a specially shaped film located directly upon a heatsink. Bismuth, which has a high Nernst—Ettingshausen coefficient $Q_\perp$, was used as the working material. The thermal flux falls on the upper surface of the film, and the magnetic flux is directed perpendicular to the thermal flux. For calculation purposes such a sensor can be represented as a thin cylinder with central orifice (Fig. 4). Such a cylinder is assumed to have ideal thermal resistance between the upper and lower surfaces and the heatsink base. Therefore, on these surfaces a constant temperature is maintained, equal to that of the surrounding medium. At the initial moment the upper cylinder surface, which is coated with a thin layer of black pigment, is subjected to a constant radiant flux. A temperature differential is thus created across the film thickness (i. e., across the cylinder height h). The sensor lateral surface exchanges heat with the surrounding medium only by radiation.

The initial and boundary conditions for this problem (Eq. (1)) in cylindrical coordinates r and z have the following form. At t = 0

$$T(0, r_0, z) = 0. \tag{16}$$

On the outer cylinder surface

$$T(t, r_0, z) = 0. \tag{17}$$

On the lower surface

$$T(t, r, 0) = 0. \tag{18}$$

On the lateral surface at any moment of time the thermal flux arriving from the cylinder volume is equal to the thermal flux radiated by the surface into the surrounding medium:

$$\left[\varkappa \frac{\partial T}{\partial z} + 4\varepsilon\sigma T_0^3 T\right]_{r=R} = 0. \tag{19}$$

On the upper surface the thermal flux incident from without is equal to the algebraic sum of the flux radiated from the surface into the surrounding space and the flux conducted into the cylinder volume:

$$\left[\varkappa \frac{\partial T}{\partial z} + 4\sigma T_0^3 T\right]_{z=h} = WE(t). \tag{20}$$

In this case for cylinder heights $h \ll \varkappa/4\sigma T_0^3$ (for Bi the quantity $\varkappa/4\sigma T_0^3 \approx 100$ cm) the sensor time constant is given by the expression

$$t_{set} = \frac{4}{\pi} \frac{cd}{\varkappa} h^2 \frac{1}{1 + \frac{64}{\pi^2} h^2 \left(\frac{\sigma T_0^3 \mu_1}{\varkappa}\right)}. \tag{21}$$

Computer calculation with Eq. (21) produced values for the time constant t_{set}. For an active bismuth layer thickness of 0.1, 1, 5, and 10 μm the corresponding time constants proved equal to $0.81\cdot10^{-9}$, $0.81\cdot10^{-7}$, $0.2\cdot10^{-5}$, and $0.81\cdot10^{-5}$ sec. The results obtained indicate that for thermomagnetic sensors in the expression for the time constant, Eq. (21), the correction in the denominator related to heat liberation by radiation is practically zero, i.e., the entire thermal flux in the sensor is determined by thermal conductivity across the active layer:

$$t_{set} \simeq \frac{4}{\pi^2} \frac{dc}{\varkappa} h^2. \tag{22}$$

For thermomagnetic sensors, there is no necessity to calculate the temperature distribution over the upper cylinder surface $T(r, h, \infty)$ to calculate the temperature distribution. Since the entire thermal flux in the sensor is determined by thermal conductivity across the active layer, i.e., $W = \varkappa\nabla T$, the voltage—current sensitivity is defined with sufficient accuracy by Eq. (15).

NOTATION

D, thermal diffusivity of active element; c, $\varkappa$, d, average specific heat, thermal conductivity, and density; c_1, $\varkappa_1$, d_1, h_1 and c_2, $\varkappa_2$, d_2, h_2, specific heat, thermal conductivity, density, and thickness of semiconductor layer and substrate respectively; r_0, radius of central disk portion; T_0, temperature of surrounding medium; R, disk radius; ε, disk emissivity; σ, Stefan−Boltzmann constant; W, radiant power incident per unit area; t_{set}, sensor time constant; x_1, first root of zeroth-order Bessel function; C, disk heat capacity; G_{rad} and G_{therm}, heat liberation coefficients related to radiation and thermal conductivity; J_0 and J_1, zeroth- and first-order Bessel functions; x_n, roots of zeroth-order Bessel function; S, voltage−power sensitivity of thermoelectric sensor; ΔT, temperature differential between "hot" and "cold" thermoelectric sensor junctions; m, number of thermoelements in sensor; $\alpha_{p,n}$, thermo−emf coefficient of individual element; F, area of sensitive region; T, temperature of surrounding medium; R, disk radius; ε, disk emissivity; E_{N-E}, U_{N-E}, electric field strength and output emf produced by Nernst−Ettingshausen effect; $Q_\perp$, transverse Nernst−Ettingshausen effect coefficient; l, h, length and height of thermomagnetic sensor working element; ∇T, temperature gradient; μ_1, first root of some dispersion equation.

LITERATURE CITED

1. D. M. Gel'fgat, Z. M. Dashevskii, N. V. Kolomoets, and I. V. Sgibnev, "Design of infrared radiation sensors using film thermoelectric materials," in: Thermoelectric Materials and Films. Materials of the All-Union Conference on Deformation and Dimensional Effects in Thermoelectric Materials and Films, Film Technology and Applications [in Russian], Leningrad Institute of Nuclear Physics (1976), pp. 240-246.
2. E. R. Washwell, S. R. Hawkins, and K. F. Cuff, "The Nernst detector: fast thermal radiation detection," Appl. Phys. Lett., 17, No. 4, 164-166 (1970).

GRAIN IN A CO_2-GDL MEDIUM WITH WEDGE AND PROFILED NOZZLES, PART I.

APPARATUS AND PULSE GAIN MEASUREMENT SYSTEM

V. A. Akimov, V. T. Karpukhin,
S. M. Chernyshev, and V. F. Sharkov

UDC 621.375.826

The apparatus is described together with the gain-measurement scheme. Weak shock waves are identified in the flow picture and probe locations are defined that are free from local inhomogeneity.

The weak-signal gain k_0 is one of the most important laser parameters [1]. Determination of the maximum gain constitutes a multifactor optimization on the stagnation parameters, the molar composition of the working mixture, and the geometrical dimensions and profile of the supersonic GDL nozzle. The nozzle produces the supersonic flow in the cavity, and its design features are sources of various gasdynamic inhomogeneities: shock waves, hot boundary layers, and wakes behind the edges. All these factors influence the state of inversion in the active medium and may increase or decrease the gain in accordance with the various line-broadening mechanisms [2].

There are many papers (see [1, 3] for reviews) on the theoretical and experimental multifactor optimization of the gain, and recently there have been papers [4-6] concerned with calculation and measurement for k_0 in a flow of a markedly inhomogeneous gas containing solid particles and shock waves.

There are several methods of measuring k_0 [7]. The maximum-loss method is based on measuring the absorption of calibrated attenuators introduced into the cavity that cut off the lasing, and the magnitude of the loss is identified with the gain. This method requires high accuracy in measuring the introduced loss and does not make allowance for the line width, which substantially reduces the accuracy in determining k_0. The